JACS
JOURNAL OF THE AMERICAN CHEMICAL SOCIETY

ARTICLE

pubs.acs.org/JACS

Proton Delivery to Ferryl Heme in a Heme Peroxidase: Enzymatic Use of the Grotthuss Mechanism

Igor Efimov,[†] Sandip K. Badyal,[‡] Clive L. Metcalfe,[†] Isabel Macdonald,[†] Andrea Gumiero,[†,‡] Emma Lloyd Raven,[*,†,§] and Peter C. E. Moody[*,‡,§]

[†]Department of Chemistry, Henry Wellcome Building, University of Leicester, University Road, Leicester LE1 7RH, England

[‡]Department of Biochemistry, Henry Wellcome Building, University of Leicester, Lancaster Road, Leicester LE1 9HN, England

Supporting Information

ABSTRACT: We test the hypothesized pathway by which protons are passed from the substrate, ascorbate, to the ferryl oxygen in the heme enzyme ascorbate peroxidase (APX). The role of amino acid side chains and bound solvent is demonstrated. We investigated solvent kinetic isotope effects (SKIE) for the wild-type enzyme and several site-directed replacements of the key residues which form the proposed proton path. Kinetic constants for H_2O_2-dependent enzyme oxidation to Compound I, k_1, and subsequent reduction of Compound II, k_3, were determined in steady-state assays by variation of both H_2O_2 and ascorbate concentrations. A high value of the SKIE for wild type APX ($^{D}k_3 = 4.9$) as well as a clear nonlinear dependence on the deuterium composition of the solvent in proton inventory experiments suggest the simultaneous participation of several protons in the transition state for proton transfer. The full SKIE and the proton inventory data were modeled by applying Gross−Butler−Swain−Kresge theory to a proton path inferred from the known structure of APX. The model has been tested by constructing and determining the X-ray structures of the R38K and R38A variants and accounts for their observed SKIEs. This work confirms APX uses two arginine residues in the proton path. Thus, Arg38 and Arg172 have dual roles, both in the formation of the ferryl species and binding of ascorbate respectively and to facilitate proton transfer between the two.

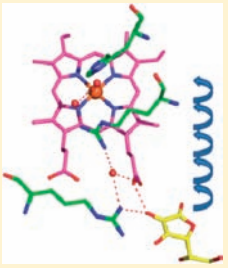

INTRODUCTION

Activation of oxygen is a classic feature of the chemistry of heme enzymes. Oxygen activation by a heme group is achieved through formation of a high-valent Compound I (ferryl) heme species, which is an intermediate in a number of well-known heme enzymes (e.g., the cytochrome P450s, nitric oxide synthases, cytochrome *c* oxidases, and the heme peroxidases) and most likely also features in the reactivity of other heme systems which are, so far, less well characterized. There are different routes for formation of Compound I that are used in different enzymes. The most direct is reaction with hydrogen peroxide, releasing water (in, for example, the heme peroxidase enzymes); the other is initial reaction of ferrous iron with dioxygen followed by a further reduction by a suitable reductase (in, for example, the P450s and NO synthase). In all cases, turnover of the enzyme depends on rereduction of Compound I with the concomitant release of 1 mol equiv of water. As well as electrons, this also requires two protons. On the whole, however, our understanding of the detailed mechanisms underpinning these proton transfers in heme proteins is very poorly formulated and lags a long way behind our understanding of Compound I itself. This is in part because structural information for representative enzyme/substrate complexes has been slow to emerge and because structural characterization of the relevant Compound I intermediates has been equally challenging.

The heme peroxidases provide a useful test bed in this context. For these enzymes the overall processes of electron and proton transfer are well-established (eqs 1−3),[1,2]

$$Fe^{III} + H_2O_2 \xrightarrow{k_1} Fe^{IV}{=}O, P^{\bullet+} + H_2O \quad (1)$$

$$Fe^{IV}{=}O, P^{\bullet+} + HS \xrightarrow{k_2} Fe^{IV}{=}O + S^{\bullet} \quad (2)$$

$$Fe^{IV}{=}O + HS \xrightarrow{k_3} Fe^{III} + S^{\bullet} + H_2O \quad (3)$$

where HS represents a generic protonated substrate that can deliver one electron and one proton (equivalent to $H^{\bullet}$) and P represents porphyrin. There is hardly any mechanistic information on how protons are transferred in any heme peroxidase, and it is important to address this deficiency. We have previously defined the binding orientations of numerous small substrates bound to ascorbate peroxidase[3−7] and have found that different substrates bind in different places, with ascorbate binding at the so-called γ-heme edge and aromatic substrates binding at the δ-heme edge. This is helpful because it has allowed us to propose[4,7] a pathway for proton transfer involving Arg172, the heme propionate, Arg38, and two water molecules (Figure 1). In this work, we have used the proton inventory method together with crystallography and solvent isotope effects to dissect this proton transfer process in detail and to examine the individual roles of key residues (Arg172, Arg38). Together with emerging information on the structures of Compound I and Compound II in the heme peroxidases,[8,28,35] this provides a more detailed picture of the proton transfer mechanism.

Received: January 24, 2011
Published: August 05, 2011

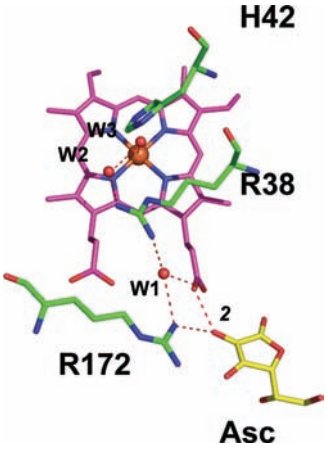

Figure 1. Structure of the ferric APX−ascorbate complex,[6] showing the hydrogen bonds which comprise the proposed[4,7] proton transfer pathway. The C^2−OH group of the ascorbate and the heme-6-propionate group are labeled. There is an additional hydrogen bond from the C^3−OH group of the ascorbate to Arg172,[6] but this is not shown since it is not part of the proposed proton transfer pathway. W3 is in the approximate position of the ferryl oxygen in Coumpound II.[8]

EXPERIMENTAL PROCEDURES

Deuterium oxide (99.9% purity) was acquired from Sigma and not purified further. L-Ascorbic acid (Aldrich Chemical Co.) and all buffers (Fisher) were all of the highest analytical grade (99%+ purity) and used without further purification.

Site-directed mutagenesis on recombinant soybean cytosolic APX (rsAPX) was performed according to the Quikchange protocol (Stratagene Ltd., Cambridge, U.K.). The wild type protein and all variants were purified as described elsewhere.[9,10] Enzyme purity was assessed using the R_z (A_{soret}/A_{280}) value (which was between 1.9 and 2.1 in each case). Purified samples of ferric R38K showed wavelength maxima at 407, 525, and ≈630 nm; for R38A, these maxima were at 403, 525, and 630 nm (for rsAPX, the maxima are at 407, 525, and ≈630 nm[11]). Absorption coefficients for R38K and R38A were determined using the pyridine-hemochromogen method[12] as ε_{407} = 107 mM^{-1} cm^{-1} and ε_{403} = 97 mM^{-1} cm^{-1}, respectively.

Steady-state measurements (50 mM potassium phosphate, pH 7.0, 25.0 °C) for oxidation of ascorbate were carried out according to published protocols[11] using the decrease in absorbance at 297 nm. The absorption coefficient of ascorbate in aqueous 0.1 M potassium phosphate at pH 7.0 is ε^H (297 nm) = 1.0 mM^{-1} cm^{-1}; in D_2O at pD 6.6, ε^D (297 nm) = 0.9 mM^{-1} cm^{-1}. The measured rates have therefore been appropriately corrected. Concentrations of enzyme in the assay were adjusted allowing for the different activities in order to obtain linear kinetics at low concentrations of substrate, that is, fairly low for more active enzymes (4.5 nM for rsAPX) and higher for less active variants (50 nM for R38A, R38K). Absorbance values were corrected for the disproportionation of substrate, according to the methods described earlier.[4] Acidity was adjusted to pH 7.0 for water and pD 6.6 for D_2O by mixing stock solutions of 0.1 M K_2HPO_4 and 0.1 M KH_2PO_4 dissolved in H_2O or in D_2O (since pH = pD + 0.4, so that the solutions in both H_2O and D_2O are at equivalent pH, this correction is used throughout). The enzyme's activity is insensitive to pH in the region of pH 7 (±1 unit).[13] Enzyme preparations were preincubated in the chosen H_2O/D_2O mixture for 1 h prior to taking kinetic measurements.

Crystals of R38A and R38K were prepared by vapor diffusion with Li_2SO_4 in the manner described earlier.[6] In each case, diffraction data were collected by the rotation method.[14] Crystals were cooled to 100 K in a stream of boiled-off nitrogen using an Oxford Cryosystems Cryostream 600 instrument. An initial exposure was used to determine the optimal data collection strategy using the autoindexing and strategy routines within MOSFLM,[15] and 90 oscillations of 1° were taken using an RAXIS-IV image plate device mounted on an RU2HB rotating anode X-ray generator with a copper target (Rigaku/MSC, The Woodlands, TX). Diffraction data were measured using MOSFLM[15] and scaled with SCALA.[16] For the subsequent calculation of R_{free},[17] 5% of the data were flagged. Rigid-body refinement using REFMAC5[16,18] was used to orient the wild-type model (PDB ID 1OAG) and SIGMA-weighted and difference maps calculated[16,19] and inspected with COOT.[20] This allowed the adjustment of the structure for the engineered mutations. Subsequent refinement and rebuilding cycles were undertaken with REFMAC5[16,18] and COOT.[20]

Table 1. Data Collection and Refinement Statistics for the Variants Examined in This Work

	protein	
	R38A	R38K
	data collection	
space group	$P4_22_12$	$P4_22_12$
cell dimensions (Å)	$a = b = 82.1$, $c = 75.0$	$a = b = 82.5$, $c = 75.0$
range of spacing (Å)[a]	41.0−1.9 (2.0−1.9)	27.2−1.90 (2.0−1.9)
total no. of observations	72 041 (9941)	71 932 (10 040)
no. unique reflections	21 100 (3013)	20 947 (2968)
$I/\sigma I$	26.5 (4.8)	17.8 (3.6)
completeness (%)	99.8 (99.7)	99.9 (99.7)
R_{merge}	0.055 (0.289)	0.045 (0.217)
	refinement statistics	
Rwork	0.152	0.175
Rfree	0.207	0.241
rms devation from ideal bonds (Å)	0.014	0.016
angles (deg)	1.41	1.39
PDB code	2Y6A	2Y6B

[a] Values in parentheses refer to the outer shell.

RESULTS

Protein Crystallography. These experiments were designed to test the model of proton transfer[4,7] in the structure shown in Figure 1. To ensure the construction of site-directed variants does not cause secondary structural changes and to aid the detailed analysis of the proton transfer pathways, structures of the R38K and R38A variants have been determined and refined; the relevant statistics are shown in Table 1. These structures and the $2F_O-F_C$ electron density maps (blue) of the residues discussed here are shown in Figure 2. The side chains and solvent molecules are defined, showing the effects of the mutations on the structure. The overall structure of the R38K variant is very similar to the wild type enzyme; however, the smaller lysine residue is flexible and the structure (Figure 2A) clearly shows a second conformation of the side chain of Lys38. Because of this, this variant cannot simultaneously accommodate the two water molecules that are visible in the active site of the wild type enzyme (shown as W2 and W3 in Figure 1 for the wild type), and only one water molecule is left on the proton pathway for R38K, which is shown as W1 in Figure 2A.

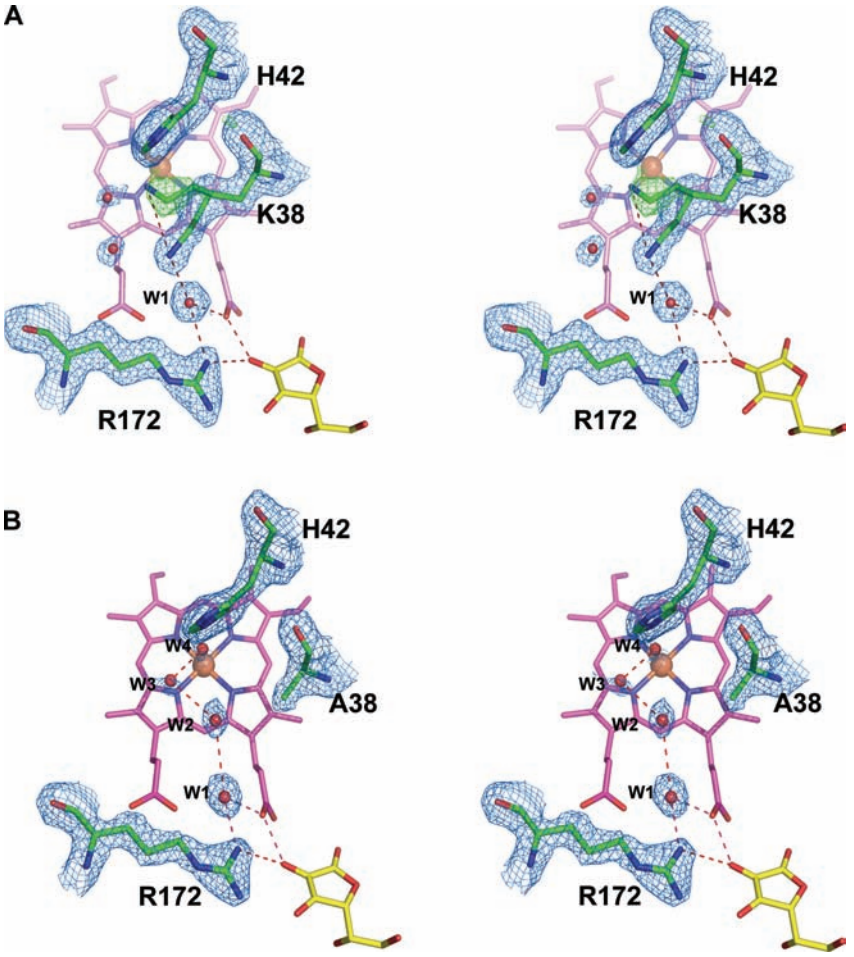

Figure 2. Structures of (A) R38K and (B) R38A. Electron densities calculated with coefficients $2F_O-F_C$ and F_O-F_C are shown in blue and green, respectively. Ordered water molecules (W1, W2, W3, W4, red spheres) are indicated. The ascorbate molecule shown (A) and (B) has been modeled into the structure of the R38K and R38A variants, based on the equivalent location in the wild type enzyme (Figure 1). Hydrogen bonding interactions are indicated with dashed lines. In panel (A), two positions of the flexible Lys38 residue are observed, with the second position shown by the F_O-F_C density.

The overall structure of R38A, Figure 2B, is again very close to that of the wild type, with one additional water (W2) in place of guanidinium group of Arg38. The hydrogen bonding arrangement suggests that this water is likely to be involved in the proton transfer pathway, which for R38A includes the three water molecules indicated in Figure 2B. These structures are considered in our kinetic analyses.

Steady State Analyses. The overall reaction scheme for APX is according to eqs 1−3. Microscopic rate constants (k_1, k_2, and k_3) in the reaction scheme have been previously determined in stopped flow experiments using single (k_1) or double (k_2 and k_3) mixing stopped flow experiments.[4,11,21] Examination of kinetic isotope effects using stopped flow is not straightforward because each stage has its own solvent isotope effect; in consequence, the delay time used in double mixing experiments depends on completion of the previous reaction step and will be different for solutions of various D_2O content. Also, for some variants, the magnitude of k_1 becomes comparable with k_3 in D_2O, which invalidates observations derived from sequential mixing experiments. To avoid these complications, and to obtain rate constants that can be reliably compared across all variants and in all solvent mixtures, a steady state assay in which both ascorbate and hydrogen peroxide concentrations are varied has been used instead.

The steady state rate, V, when $k_2 \gg k_3$[11] (k_2 involves only electron transfer and is expected to be fast, whereas k_3 involves both electron and proton transfer and is slower), is expressed by eq 4[22] (where E = enzyme, HS = ascorbic acid).

$$V = \frac{2k_1k_3[E][HS][H_2O_2]}{k_1[H_2O_2] + k_3[HS]} \quad (4)$$

Hence, by variation of both ascorbate and H_2O_2 concentrations, it is possible to determine values for k_1 and k_3 with high accuracy in mixtures of H_2O/D_2O. Primary (Figure 3A, C) and secondary (Figure 3B, D) Lineweaver−Burk plots of the reaction rate as a function of concentration of both ascorbate and H_2O_2 in steady state assays with rsAPX were carried out in both H_2O (Figure 3A, B) and D_2O (Figure 3C, D).[23] The primary plots (Figure 3A, C) show strictly parallel lines; a linear dependence passing through the origin is also observed in the secondary plots (Figure 3B, D). This confirms the validity of eq 4 for the reaction mechanism, which predicts that plots of $1/V$ versus $1/[HS]$ are linear with the same slope. The primary plots allow determination of the microscopic rate constant k_3 in H_2O ($k_{3,H} = 2.0 \pm 0.1 \times 10^5$ M^{-1} s^{-1}, Figure 3A) and the corresponding value, $k_{3,D}$, in D_2O ($k_{3,D} = 4.1 \pm 0.2 \times 10^4$ M^{-1} s^{-1}, Figure 3C). The value for the

dx.doi.org/10.1021/ja2007017 |J. Am. Chem. Soc. 2011, 133, 15376–15383

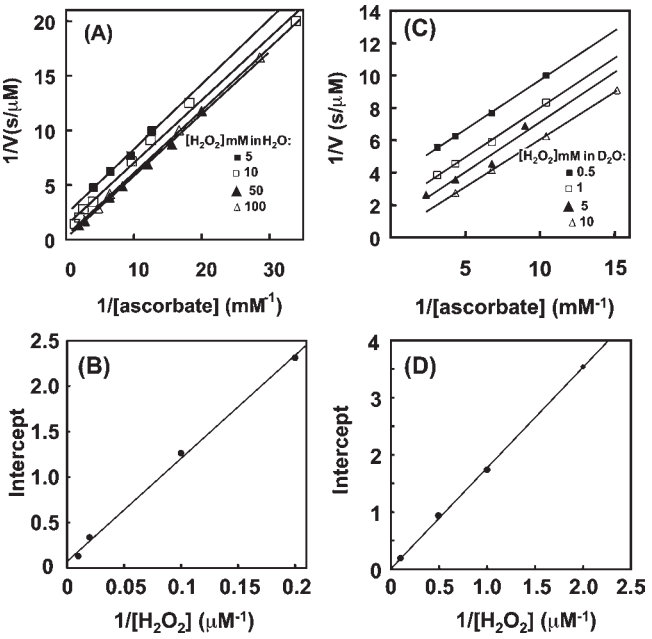

Figure 3. Steady state kinetic data for ascorbate oxidation by rsAPX in H_2O (A, B) and D_2O (C, D). For primary Lineweaver–Burk plots, reciprocal rates are shown as functions of reciprocal ascorbate concentrations at constant H_2O_2 concentration for each line, which is indicated on the plot; experiments in both H_2O (A) and D_2O (C) are indicated. Secondary Lineweaver–Burk plots, in which the intercepts from the linear fits in (A) and (C), respectively, are plotted as a function of reciprocal H_2O_2 concentration are shown in (B) and (D), respectively. Ascorbate oxidation was calculated from a decrease of absorbance at l = 290 nm, using $e = 1\ mM^{-1}\ cm^{-1}$. Conditions: 50 mM KPi, pH 7, 25.0 °C, [enzyme] = 4 nM. Plots against ascorbate were corrected for the change in absorption coefficient of ascorbate in D_2O (see Experimental Procedures).

Table 2. Summary of Kinetic Constants ($M^{-1}\ s^{-1}$) Derived in This Work ($k_{1,H}$ and $k_{3,H}$ Measured in H_2O; $k_{1,D}$ and $k_{3,D}$ Measured in D_2O) and Derived Values of $^Dk_1$ and $^Dk_3$[a]

enzyme	$k_{1,H}$	$k_{1,D}$	$^Dk_1$	$k_{3,H}$	$k_{3,D}$	$^Dk_3$
rsAPX	1.0×10^7	1.3×10^7	0.8	2.0×10^5	4.1×10^4	4.9
R38A	6.0×10^5	9.0×10^4	6.6	6.0×10^5	1.3×10^5	4.6
R38K	8.5×10^6	3.8×10^6	2.2	4.4×10^5	3.1×10^5	1.4
R172K	3.9×10^5	3.1×10^5	1.3	1.6×10^4	7.7×10^3	2.1

[a] Error is 10% for all values.

isotope effect, $^Dk_3 = k_{3,H}/k_{3,D} = 4.9$, can thus be derived. The observed value is quite high compared to a typical solvent kinetic isotope effect of 2.0 for a single proton and is consistent with the concerted movement of several protons. This is discussed below. Further, from the slopes of the secondary plots (Figure 3B, D), which are equal to $(2k_1[E])^{-1}$, $k_{1,H} = (1.03 \pm 0.05) \times 10^7\ M^{-1}\ s^{-1}$ for H_2O and $k_{1,D} = (1.32 \pm 0.06) \times 10^7\ M^{-1}\ s^{-1}$ for D_2O, with $^Dk_1 = k_{1,H}/k_{1,D} = 0.78$. Data obtained in this way for the wild type enzyme, rsAPX, are presented in Table 2.

We have used the same analysis to examine a number of other variants which are expected to perturb the proposed proton pathway (R172K, R38A, R38K variants). Corresponding data for all of these variants are also presented in Table 2.

Proton Inventories. The proton inventory method, in which the ratios of solvent (H_2O, D_2O) are varied, allows kinetic assessment of the proton transfer mechanism from examination of the dependence of reaction rate as a function of the fraction of D_2O in solution.

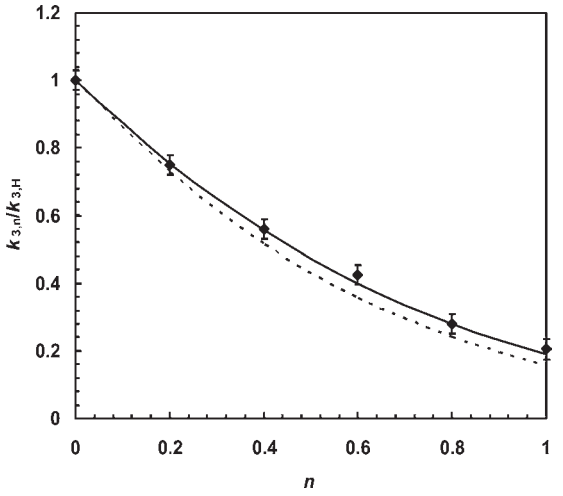

Figure 4. Proton inventory data for rsAPX. $k_{3,n}/k_{3,H}$ denotes $k_{3,n}$ measured at $n = [D_2O]/([D_2O] + [H_2O])$ divided by $k_{3,H}$ (measured in H_2O). Kinetic constants were determined in steady state assays where [enzyme] = 10 nM, $[H_2O_2]$ = 100 mM, [ascorbate] = 600 mM, and n is varied between 0 and 1. The solid line is a fit of the data to eq A26 in the Supporting Information using literature values $l = 0.69$, $\varphi^{NH} = \varphi^{NH2} = 0.92$, $\varphi^{NH3} = 0.97$. The dashed line is calculated considering only water molecules $k_{3,n}/k_{3,H} = (1 - n + nl)^5$. Conditions: 50 mM potassium phosphate buffer, pH 7.0, 25 °C.

Figure 4 shows proton inventory data measured for k_3 for rsAPX only. We report values for $k_{3,n}$, which is k_3 measured under conditions where the fraction of D_2O in the solvent (H_2O) varies and is defined by n (where $n = [D_2O]/([D_2O] + [H_2O])$). As shown in Figure 4, $k_{3,n}$ decreases nonlinearly with increasing concentrations of D_2O to a final value that is approximately 20% of that in pure H_2O. As was the case for the steady state data above, this nonlinearity also suggests participation of several protons in the transition state.[24] This is discussed in detail below, together with the roles of individual residues in this proton transfer process.

Analysis of the Proton Transfer Pathway during Substrate Oxidation. The above kinetic data, from both steady state and proton inventory analyses, indicates the participation of more than one proton in the transition state. The proton transfer pathway is analyzed further here with reference to the rate constants obtained for k_3 in either H_2O or D_2O. In our analyses, we have assumed that ascorbate is anionic in solution (pK_a of C^3–OH = 4.0, Scheme 1); one-electron oxidation gives the protonated monodehydroascorbate radical which has a C^2–OH group which is much more acidic ($pK_a = -0.45$) than that in the original anionic form ($pK_a = 11.3$) and will thus rapidly deprotonate (Scheme 1). From the structure of the ferric APX–ascorbate complex (Figure 1), we conclude that upon oxidation of the substrate one proton is transferred from the 2-OH group of ascorbate ($pK = -0.45$ in water[25]) to Arg172, another from Arg172 to the ordered water molecule W1, and a third from Arg38 to the ordered water molecule W2 in a concerted manner and finally to the ferryl oxygen, whose approximate position[8] is shown by W3. In this way, we model a transition state that consists of a deprotonated Arg38, Arg172, and two protonated water molecules (W1 and W2). This assumption is supported by our recent neutron diffraction

Scheme 1. Chemistry of Ascorbate,[55−57] Showing Relevant Reduction Potentials[a]

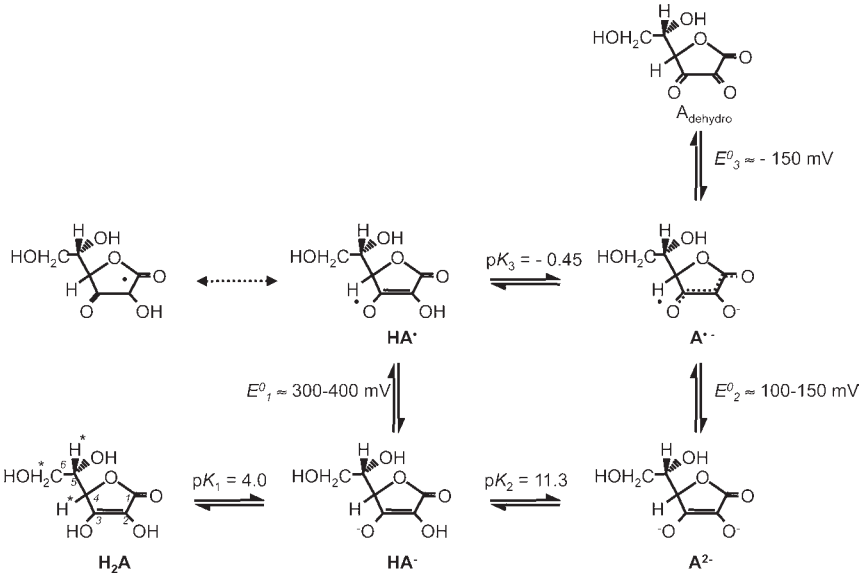

[a] The doubly protonated form (AH_2) is readily deprotonated in water at neutral pH (pK_a of C^3−OH = 4.0) to give the anionic form (AH^-). Binding of AH^- to APX and one-electron oxidation by Compound I/II leads to the mondehydroascorbate radical ($AH^•$) which is very acidic. This radical thus readily deprotonates at the C^2−OH group (pK_a = −0.45) and transfers a proton to Arg172 (Figure 1), which initiates the sequence of concerted proton transfers discussed in this paper and leads ultimately to protonation of Compound II.

studies of the related heme peroxidase cytochrome *c* peroxidase enzyme (unpublished) which confirms that the protons of the residue positioned equivalently to Arg38 (Arg48) are exchangeable with the deuterium in D_2O.

Theoretical analysis of deuterium/protium equilibria has been of long-standing interest, as reflected in quite early literature,[26−28] and below we describe such an analysis for the proton inventory data presented above. All of the necessary derivations are provided in the Supporting Information. The resulting eq 5, which is eq A26 in the Supporting Information, describes the analysis of proton inventory data for the case of a simultaneous transfer of three protons:

$$\frac{k_{3,\mathrm{H}}^{\mathrm{rsAPX}}}{k_{3,\mathrm{n}}^{\mathrm{rsAPX}}} = \frac{k_{\mathrm{H}}^{\mathrm{asc}}}{k_{\mathrm{n}}^{\mathrm{asc}}}\left(\frac{k_{\mathrm{H}}}{k_{\mathrm{n}}}\right)^2 = \frac{(1-n+n\varphi^{\mathrm{NH2}})^5}{(1-n+nl)^5(1-n+n\varphi^{\mathrm{NH3}})^2(1-n+n\varphi^{\mathrm{NH}})^2} \quad (5)$$

where the notations l and φ are the fractionation factors (defined in the Supporting Information) which report, respectively, on the equilibrium protonation/deuteration processes for the solvent molecules (eqs A1 and A2) and arginine residue (eq A18) involved. Analysis of this model (see Supporting Information eqs A22−A26) shows that the most important contribution to the dependence of the SKIE on the D_2O content, n, comes from the fractionation factor of water l and is proportional to $\sim(1-n+nl)^{-5}$ in eq 5.[29] The experimental proton inventory data for rsAPX have been fitted to eq 5 using established literature values[24,30] for l (= 0.69) and $\varphi^{\mathrm{NH}} = \varphi^{\mathrm{NH2}}$ (= 0.92), and φ^{NH3} (= 0.97). Although there may be medium effects in a complex enzymatic process and thus the combined influence of multiple small changes of fractionation factors of solvent in the transition state compared with ground state may be significant,[31] there is nevertheless a good correlation between the data and eq 5 (Figure 4), showing agreement with the assumptions regarding the transition state, and the involvement of three protons. The same figure also shows the calculation considering only water molecules, i.e. $k_{3,\mathrm{n}}/k_{3,\mathrm{H}} = (1-n+nl)^5$. This shows that contribution from φ^{NH},φ^{NH2}, φ^{NH3} fractionation factors is small, but not negligible.

The structure of the enzyme constrains the possible proton pathways, and the proposed pathway is consistent with the analysis afforded by eq 5. The fractionation factors for NH bonds are close to 1, and thus, the inventory curve (Figure 4) reflects only the fractionation factors for water molecules and the theoretical formula is close to single exponent with n = 5. Thus, the choice of proton path is restricted by the available water molecules, whose locations are known from structure. Consequently, the solvent isotope effect is defined by a number of participating O−H bonds (fractionation factor of 0.69), whereas N−H bonds are again added by necessity from the structure. This allows determination of the unique path. In the case of mutations (below), only the total isotope effect is analyzed.

To calculate a full isotope effect for rsAPX (i.e., in 100% D_2O), by making n = 1 in eq 5. This leads to eq 6.

$$\frac{k_{3,\mathrm{H}}^{\mathrm{rsAPX}}}{k_{3,\mathrm{D}}^{\mathrm{rsAPX}}} = \frac{(\varphi^{\mathrm{NH2}})^5}{l^5(\varphi^{\mathrm{NH3}})^2(\varphi^{\mathrm{NH}})^2} \quad (6)$$

This leads to a calculated value for $k_{3,\mathrm{H}}/k_{3,\mathrm{D}}$ for rsAPX of 5.29, which is very close to the experimentally measured value of 4.9 (Table 2). The agreement of these values is consistent with the proton inventory analysis above and indicates that the unexpectedly large SKIE of 4.9 corresponds to a transition state in which three protons are transferred simultaneously, two of which reside on ordered waters W1 and W2 (forming two H_3O^+, Figure 1).[32]

In the following analyses, we further dissect the proton transfer pathway, by examination of the individual role of key residues.

The Role of Arg172. The structure R172K is not available, but for the purposes of this analysis and by analogy with the structures of R172A[4] and R38A (Figure 2A), in which the void volume is occupied by water molecules in both cases, we have assumed that a water molecule also occupies the space vacated by the (bulkier) Arg172 side chain in the R172K variant. In this case, the SKIE for R172K arises from (assumed to be rate-limiting) transfer of the proton from the C^2−OH group on ascorbate to this water molecule but the overall process is not fully concerted because of the mutation. In this case, the fractionation factor would be l^1 (= l) arising from transfer of the single proton from the C^2−OH bond of the ascorbate to an adjacent water molecule. In this case, eq 5 reduces to eq 7 because Arg172 is missing and is replaced by a water molecule (see eqs A27 and A28, Supporting Information):

$$\frac{k_{3,\mathrm{H}}^{\mathrm{R172K}}}{k_{3,\mathrm{D}}^{\mathrm{R172K}}} = \frac{l}{l^3} \tag{7}$$

This leads to a calculated value for $k_{3,H}/k_{3,D}$ for R172K of 2.1, which is in agreement with the experimental value ${}^{D}k_3$ = 2.1 (Table 2). This confirms our analyses and shows that the concerted process is interrupted by the Arg172 mutation.

The Role of Arg38. We have examined two variants, R38K and R38A, the structures for both of which are shown (Figure 2). Inspection of Table 2 reveals that the R38K variant has a SKIE effect (${}^{D}k_3$) that is significantly smaller (${}^{D}k_3$ = 1.4) than that for rsAPX (${}^{D}k_3$ = 4.9). Values for the SKIE of less than 3, which correspond to a situation where $l^{-3} = (0.69)^{-3} = 3$, are a result of the participation of only one water molecule, which again suggests that the concerted mechanism is disrupted. As explained above, the lysine side chain is mobile in the R38K structure and only one conserved water molecule is visible in the structure when compared to rsAPX (Figure 2A). In this case, the full solvent isotope effect for R38K is obtained from eq 6 by removing the fractionation factor l^3 for water, which is missing in the structure, from the denominator, as well as by removing all terms for Arg38 (eq 8).

$$\frac{k_{3,\mathrm{H}}^{\mathrm{R38K}}}{k_{3,\mathrm{D}}^{\mathrm{R38K}}} = \frac{(\varphi^{\mathrm{NH2}})^3}{l^2(\varphi^{\mathrm{NH3}})^3\varphi^{\mathrm{NH}}} \tag{8}$$

This gives a calculated value of 1.95, which compares well to the experimental value ($k_{3,H}/k_{3,D}$) of 1.4 (Table 2). This demonstrates that proton transfer in this case is disrupted by the Arg38 mutation and is thus not concerted. Interestingly, the data in Table 2 for R38A also show differences in relative effect of the mutation on k_1 and k_3, with values of $k_{1,H} \approx 17$ times lower than rsAPX and values for $k_{3,H}$ approximately the same as those for rsAPX. The lower value of $k_{1,H}$ is most likely due to the absence of potential hydrogen bonding interactions, either to the bound ferric−peroxide complex (which is too transient to detect) or in the resulting Compound I species (the X-ray structure shows the oxygen atom of Fe(IV)═O is within hydrogen bond distance of the guanidinium of Arg38).[8]

According to Table 2, R38A has a SKIE ($k_{3,H}/k_{3,D}$) closer to the wild type value. The crystal structure (Figure 2B) confirms that the smaller Ala side chain allows accommodation of another water molecule (W2) in the active site which is not present for the R38K variant. Proton transfer between water molecules does not contribute to the measured solvent isotope effect, because the initial and final states in eq A6 (Supporting Information) are the same. Therefore, the expression for the full SKIE is different from that for rsAPX by factors attributable only to the guanidine group of Arg38, eq 9:

$$\frac{k_{3,\mathrm{H}}^{\mathrm{R38K}}}{k_{3,\mathrm{D}}^{\mathrm{R38K}}} = \frac{(\varphi^{\mathrm{NH2}})^2}{l^5(\varphi^{\mathrm{NH3}})^2\varphi^{\mathrm{NH}}} \tag{9}$$

In this case, the calculated theoretical value of $k_{3,H}/k_{3,D}$ = 6.25 which is in reasonable agreement with the experimentally observed value of 4.6 (Table 2). The difference may be due to the movement of the three protons not being fully concerted, which is assumed in the derivation, or a function of the additional positional freedom of the water molecules.

Analysis of Proton Transfer in Compound I Formation. The steady state analyses presented in Figure 3 also generate calculated values for the k_1 microscopic constants (Table 2). We are therefore able to extract isotope effects for the first stage of the catalytic cycle (i.e., the dependence of k_1 on solvent), and our analyses as described above for k_3 allows rationalization within the same framework.

According to Table 2, ${}^{D}k_1$ = 0.8 for rsAPX. If the rate-determining step is transfer of hydrogen from the bound peroxide to His42, then the following equilibrium defines the SKIE:

$$\mathrm{His{-}N} + \mathrm{H{-}O{-}O{-}H\cdots Fe} \leftrightarrow [\mathrm{His{-}NH^{+}\cdots {}^{-}O{-}O{-}H\cdots Fe}] \tag{10}$$

where H−O−O−H···Fe denotes peroxide in active site, His-N denotes His42, and His-NH^+ is the protonated form of His42.. = Applying the same rules as derived in the Supporting Information, we the obtain SKIE as follows:

$$\frac{k_{1,\mathrm{H}}^{\mathrm{rsAPX}}}{k_{1,\mathrm{D}}^{\mathrm{rsAPX}}} = \frac{l}{\varphi^{\mathrm{NH}}} = 0.75 \tag{11}$$

which agrees well with the experimental value of ${}^{D}k_1$ = 0.8, confirming that the rate limiting step is a protonation event. This step may be water-mediated as described for HRP and analyzed with density functional theory,[33] but this would not affect our calculation because the corresponding fractionation factors to an intermediate water would cancel out. The R172K mutation would not be expected to affect the mechanism of Compound I formation (because R172 is not in the heme active site), and so it follows logically that the SKIE for k_1 in this variant would be close to the value obtained for rsAPX; as expected, the experimental value of ${}^{D}k_1$ = 1.3 for R172K in fact is close to that for rsAPX (0.8).

The Arg38 variants do, however, affect the SKIE dependence of k_1, with values for ${}^{D}k_1$ of 2.2 and 6.6, respectively, for R38K and R38A. Since the values for $k_{1,H}$ and $k_{1,D}$ for R38K are both lower than those for rsAPX, we assume that transfer of proton from peroxide to His42 as described above (eq 10) is no longer rate-limiting. In this variant, the structure permits the accommodation of an additional water molecule in the space opened by the flexible Lys38 side chain, so we suggest that the rate-limiting step is, instead, proton transfer from peroxide and this proceeds via this additional water molecule and eq 10 should be adjusted as follows:

$$\mathrm{H_2O} + \mathrm{H{-}O{-}O{-}H\cdots Fe} = [\mathrm{H_3O^{+}\cdots {}^{-}O{-}O{-}H\cdots Fe}] \tag{12}$$

In this case, SKIE would be

$$\frac{k_{1,\mathrm{H}}}{k_{1,\mathrm{D}}} = \frac{l}{l^3} = 2.1 \tag{13}$$

which is consistent with the measured SKIE for R38K ($^{D}k_1 = 2.2$). In the case of R38A (Figure 2B), the structure shows the presence of yet another water molecule which multiplies eq 13 by the factor l^{-3}, so that

$$\frac{k_{1,H}}{k_{1,D}} = \frac{l}{l^3 l^3} = 6.4 \quad (14)$$

This agrees with the measured value for R38A ($^{D}k_1 = 6.6$) and is consistent with the involvement of Arg38 in Compound I formation.

DISCUSSION

In the peroxidase enzymes, the process of proton transfer from the substrate to Compound II and the concomitant release of water in the final step are still very poorly defined. This is in part because structural information for representative peroxidase/substrate complexes has been very slow to emerge and because the various substrates bind in a variety of positions and the most studied examples (e.g., cytochrome *c* peroxidase and manganese peroxidase) have "atypical" substrates (i.e., not a small organic molecule) and so have not provided the necessary generic insight (see ref 3 for a recent review). Furthermore, rigorous structural description of the relevant ferryl intermediates has been challenging, although important structural information is now beginning to appear.[8,34−41]

The APX−ascorbate system provides a new paradigm for small organic molecules as substrates for heme peroxidases and an opportunity to dissect proton transfer in further detail. It is notable that, aside from the heme propionates, there are no acidic residues on the proton pathway that might mediate the proton transfer process: the only possibility is proton transfer mediated by Arg172, Arg38, and intervening water molecules (Figure 1). All of the data presented in this paper support a concerted mechanism for proton transfer involving three water molecules, so that the entire proton transfer event comprises the loss of a proton from the C^2−OH group of the substrate, with the concerted transfer of protons through a path defined by two arginine residues and two solvent molecules. There are two key arginine residues identified, Arg172 and Arg38, and our data support a dual role for both. On the one hand, they are important for binding of substrate (Arg172) or peroxide (Arg38), and on the other they are intimately involved in the proton transfer pathway. Such a role for Arg38 as part of the proton delivery mechanism is consistent with the fact that it is conserved across all heme peroxidases. The transfer of protons via water molecules has been shown in human carbonic anhydrase where there is 15 Å hydrogen bonded water-mediated proton transfer "wire" from a Zn^{2+}-bound water to a histidine side chain that acts as a proton shuttle.[42] The observations recorded here are consistent with the pathway for proton transfer hypothesized from the crystal structure[4] and shown in Figure 1; furthermore, we have shown that the movement of protons is a concerted process[43] involving the simultaneous loss of a proton from the ascorbate substrate with the donation from the distal arginine to the oxy-ferryl intermediate. This concerted process whereby the addition of a proton at one end of a hydrogen-bond network results in the loss of a proton at the other end, "the Grothuss Mechanism"[43] (see ref 44 for a recent review), is analogous to the transmission of electron through metal wire.

Arg38 (Figure 1) or its equivalents is conserved in many heme enzymes, but its apparent role is limited to being a hydrogen bond donor and not a proton donor. In HRP, the substrate ferulic acid is bound close enough to heme, so that proton delivery is mediated by a single water molecule.[45−47] Arg38 of HRP (equivalently positioned) donates a hydrogen bond to the active water and to the phenolic oxygen of the substrate, but it is not deprotonated during the catalytic cycle. In this sense, APX is exceptional, because its Arg38 plays double role: it participates in binding of peroxide as a hydrogen bond donor and in reduction of Compounds I and II as a proton donor.

Arginine normally has a high pK_a (12.5) and would thus not automatically be expected to be a good proton donor; however, the protons are rapidly exchangeable in an aqueous environment and arginine is implicated as being involved in enzymatic proton transfer, for example, in fumarate reductase.[48,49] In cytochrome *c* oxidase,[50] Arg481 and Arg482 are associated with propionates of hemes a and a_3 in similar way as Arg172 is associated with the heme propionate in APX. It is supposed that those propionates participate in proton movement.

The Role of the Heme Propionates. There has been recent discussion relating to the role of heme propionates in heme reactivity.[51,52] The configuration of hydrogen bonds depicted in Figure 1 suggests that the proton relay path could equally well proceed through the heme 6-propionate. This pathway is indistinguishable by studying the isotope effect alone in rsAPX, since it also has three water molecules, which give maximal contribution to the total effect. However, the R172K mutation decreases the rate constant k_3 by an order of magnitude (Table 2), which we interpret as showing that the concerted proton transfer has been perturbed by the R172K mutation. Consequently, we conclude that in rsAPX the path is through Arg172 and not the heme propionates. The role of the heme propionates is more likely to be through hydrogen bond stabilization of the bound ascorbate;[4] similar interactions are used to hold Mn^{II} in place at the analogous site in manganese peroxidase.[53,54] This structure may allow electron transfer from the substrate to the heme through these bonds, but our data do not support a similar role in controlling proton delivery in this case.

Role of Active Site Water Molecules. All the mutations studied in this work create space filled by crystalline water. It can replace Arg38 in the active site, with slightly diminishing k_1 and increasing k_3, therefore, without dramatic changes in catalysis. This is understandable, because the distal pocket is buried inside the protein and thus confines the substrate. Replacement of the Arg172 side chain by a smaller residue (R172K, R172A[4]) also opens the ascorbate site to the bulk solvent and results in dramatically reduced activity.

This work has demonstrated the concerted pathway of proton transfer in ascorbate peroxidase catalysis and revealed the role of solvent and arginine side chains in the process.

ABBREVIATIONS

APX, ascorbate peroxidase; rsAPX, recombinant soybean cytosolic ascorbate peroxidase, HRP, horseradish peroxidase, SKIE, solvent kinetic isotope effect.

ASSOCIATED CONTENT

Supporting Information. Derivation of equations for analysis of proton inventory data. This material is available free of charge via the Internet at http://pubs.acs.org.

AUTHOR INFORMATION

Corresponding Author
emma.raven@leicester.ac.uk; peter.moody@leicester.ac.uk

Author Contributions

[§]These authors contributed equally to this work.

■ ACKNOWLEDGMENT

This work was supported by grants from BBSRC (BB/C00602X/1 to E.L.R./P.C.E.M., IIP0206/009 to E.L.R., and studentship to S.K.B.) and The Leverhulme Trust (Grant RF/RFG/2005/0299 to E.L.R./P.C.E.M. and studentship to A.G.).

■ REFERENCES

(1) Dunford, H. B. *Heme Peroxidases*; John Wiley: Chichester, 1999.
(2) Dunford, H. B. *Peroxidases and Catalases: Biochemistry, Biophysics, Biotechnology and Physiology*, 2nd ed.; John Wiley: Chichester, 2010.
(3) Gumiero, A.; Murphy, E. J.; Metcalfe, C. L.; Moody, P. C.; Raven, E. L. *Arch. Biochem. Biophys.* **2010**, *500*, 13–20.
(4) Macdonald, I. K.; Badyal, S. K.; Ghamsari, L.; Moody, P. C.; Raven, E. L. *Biochemistry* **2006**, *45*, 7808–7817.
(5) Metcalfe, C.; Macdonald, I. K.; Murphy, E. J.; Brown, K. A.; Raven, E. L.; Moody, P. C. *J. Biol. Chem.* **2008**, *283*, 6193–6200.
(6) Sharp, K. H.; Mewies, M.; Moody, P. C.; Raven, E. L. *Nat. Struct. Biol.* **2003**, *10*, 303–307.
(7) Sharp, K. H.; Moody, P. C.; Brown, K. A.; Raven, E. L. *Biochemistry* **2004**, *43*, 8644–8651.
(8) Gumiero, A.; Metcalfe, C. L.; Pearson, A. R.; Raven, E. L.; Moody, P. C. *J. Biol. Chem.* **2011**, *286*, 1260–1268.
(9) Badyal, S. K.; Joyce, M. G.; Sharp, K. H.; Seward, H. E.; Mewies, M.; Basran, J.; Macdonald, I. K.; Moody, P. C.; Raven, E. L. *J. Biol. Chem.* **2006**, *281*, 24512–24520.
(10) Metcalfe, C. L.; Ott, M.; Patel, N.; Singh, K.; Mistry, S. C.; Goff, H. M.; Raven, E. L. *J. Am. Chem. Soc.* **2004**, *126*, 16242–16248.
(11) Lad, L.; Mewies, M.; Raven, E. L. *Biochemistry* **2002**, *41*, 13774–13781.
(12) Antonini, M.; Brunori, E. *Hemoglobin and Myoglobin and their Reactions with Ligands*; North Holland Publishers: Amsterdam, 1971.
(13) Turner, D. D. Ph.D. Thesis, University of Leicester, 2000.
(14) Arndt, U. W.; Wonacott, A. J. *The Rotation Method in Crystallography*; North Holland Publishers: Amsterdam, 1977.
(15) Leslie, A. G. W. *Joint CCP4 + ESF-EAMCB Newsletter on Protein Crystallography, No. 26*, 1992.
(16) Collaborative Computational Project, N. *Acta Crystallogr.* **1994**, *D50*, 760−763.
(17) Brünger, A. T. *Methods Enzymol.* **1997**, *277*, 366–396.
(18) Murshudov, G. N.; Vagin, A. A.; Dodson, E. J. *Acta Crystallogr.* **1997**, *D53*, 240–255.
(19) Read, R. J. *Acta Crystallogr.* **1986**, *A42*, 140–149.
(20) Emsley, P.; Cowtan, K. *Acta Crystallogr.* **2004**, *D60*, 2126–2132.
(21) Lad, L.; Mewies, M.; Basran, J.; Scrutton, N. S.; Raven, E. L. *Eur. J. Biochem.* **2002**, *269*, 3182–3192.
(22) Fergusson, R. R. *J. Am. Chem. Soc.* **1956**, *78*, 741–745.
(23) Measurement of k_1 and k_3 using this steady state method has certain technical difficulties when the two rate constants are different by several orders of magnitude, as is the case here. For meaningful sampling of eq 4, concentrations of H_2O_2 and ascorbate should be chosen such that the term $k_1[H_2O_2]$ is of the same order of magnitude as $k3[HS]$. When $k_1 \gg k_3$, this means $[H_2O_2] \ll [HS]$. However, the concentration of H_2O_2 cannot be too low because the condition $[H_2O_2] \gg [enzyme]$ must also apply for the steady state to be valid. Therefore, there are a limited range of concentrations which can be used in this experiment, which results in fewer points on the plots, Figures 2, than for a normal steady state experiment, especially at low concentrations.
(24) Schowen, K. B.; Schowen, R. L. *Methods Enzymol.* **1982**, *87*, 551–606.
(25) Shriver, D. F. A., P., W. *Inorganic Chemistry*, 3rd ed.; Oxford University Press: Oxford: 1999.
(26) Purlee, E. L. *J. Am. Chem. Soc.* **1959**, *81*, 263–272.
(27) Salomaa, P.; Schaleger, L. L.; Long, F. A. *J. Am. Chem. Soc.* **1964**, *86*, 1–7.
(28) Swain, C. G.; Thornton, E. R. *J. Am. Chem. Soc.* **1961**, *83*, 3890–3896.
(29) The exponent of "−5" in this expression is due to one O−H bond in the initial state and six O−H bonds in the transition state recruited by participation of two H_3O^+ molecules
(30) Cleland, W. W. *Methods Enzymol.* **1975**, *64*, 104–125.
(31) Chang, T. K.; Chaing, Y.; Guo, H.-X.; Kresge, A. J.; Mathew, L.; Powell, M. F.; Wells, J. A. *J. Am. Chem. Soc.* **1996**, *118*, 8802–8807.
(32) We note that coupled proton transfer of this kind in a general system $A^+H\cdots BH\cdots A$ was studied theoretically some time ago. In the case where A is NH_3 and B is HOH (which corresponds most closely to a proton relay between two arginine side chains via water, as observed in APX), the path through the cationic intermediate $NH_3\cdots H_3O^+\cdots NH_3$ was found to be energetically preferable. This is consistent with our model, where two hydroxonium molecules are formed in the transition state.
(33) Vidossich, P.; Fiorin, G.; Alfonso-Prieto, M.; Derat, E.; Shaik, S.; Rovira, C. *J. Phys. Chem. B* **2010**, *114*, 5161–5169.
(34) Berglund, G. I.; Carlsson, G. H.; Smith, A. T.; Szoke, H.; Henriksen, A.; Hajdu, J. *Nature* **2002**, *417*, 463–468.
(35) Rittle, J.; Green, M. T. *Science* **2010**, *330*, 933–937.
(36) Bonagura, C. A.; Bhaskar, B.; Shimizu, H.; Li, H.; Sundaramoorthy, M.; McRee, D. E.; Goodin, D. B.; Poulos, T. L. *Biochemistry* **2003**, *42*, 5600–5608.
(37) Fulop, V.; Phizackerley, R. P.; Soltis, S. M.; Clifton, I. J.; Wakatsuki, S.; Erman, J.; Hajdu, J.; Edwards, S. L. *Structure* **1994**, *2*, 201–208.
(38) Hersleth, H. P.; Dalhus, B.; Gorbitz, C. H.; Andersson, K. K. *J. Inorg. Biochem.* **2002**, *7*, 299–304.
(39) Hersleth, H. P.; Ryde, U.; Rydberg, P.; Gorbitz, C. H.; Andersson, K. K. *J. Inorg. Biochem.* **2006**, *100*, 460–476.
(40) Murshudov, G. N.; Grebenko, A. I.; Brannigan, J. A.; Antson, A. A.; Barynin, V. V.; Dodson, G. G.; Dauter, Z.; Wilson, K. S.; Melik-Adamyan, W. R. *Acta Crystallogr., Sect. D: Biol. Crystallogr.* **2002**, *58*, 1972–1982.
(41) Meharenna, Y. T.; Doukov, T.; Li, H.; Soltis, S. M.; Poulos, T. L. *Biochemistry* 2010, *49*, 2984–2986.
(42) Domsic, J. F.; Williams, W.; Fisher, S. Z.; Tu, C.; Agbandje-McKenna, M.; Silverman, D. N.; McKenna, R. *Biochemistry* **2010**, *49*, 6394–6399.
(43) Grotthuss, C. J. T. *Ann. Chim.* **1806**, *58*, 54–73.
(44) Wraight, C. A. *Biochim. Biophys. Acta* **2006**, *1757*, 886–912.
(45) Derat, E.; Shaik, S. *J. Am. Chem. Soc.* **2006**, *128*, 13940–13949.
(46) Derat, E.; Shaik, S.; Rovira, C.; Vidossich, P.; Alfonso-Pietro, M. *J. Am. Chem. Soc.* **2007**, *129*, 6346–6347.
(47) Henriksen, A.; Smith, A. T.; Gajhede, M. *J. Biol. Chem.* **1999**, *274*, 35005–35011.
(48) Pankhurst, K. L.; Mowat, C. G.; Rothery, E. L.; Hudson, J. M.; Jones, A. K.; Miles, C. S.; Walkinshaw, M. D.; Armstrong, F. A.; G.A., R.; Chapman, S. K. *J. Biol. Chem.* **2006**, *281*, 20589–20597.
(49) Taylor, P.; Pealing, S. L.; Reid, G. A.; Chapman, S. K.; Walkinshaw, M. D. *Nat. Struct. Biol.* **1999**, *6*, 1108–1112.
(50) Mills, D. A.; Geren, L.; Hiser, C.; Schmidt, B.; Durham, B.; Millett, F.; Ferguson-Miller, S. *Biochemistry* **2005**, *44*, 10457–10465.
(51) Poulos, T. L. *Nat. Prod. Rep.* **2007**, *24*, 504–510.
(52) Guallar, V.; Olsen, B. *J. Inorg. Biochem.* **2006**, *100*, 755–760.
(53) Sundaramoorthy, M.; Kishi, K.; Gold, M. H.; Poulos, T. L. *J. Biol. Chem.* **1994**, *269*, 32759–32767.
(54) Sundaramoorthy, M.; Youngs, H. L.; Gold, M. H.; Poulos, T. L. *Biochemistry* **2005**, *44*, 6463–6470.
(55) Bryan, D. M.; Dell, S. D.; Kumar, R.; Clarke, M. J.; Rodriguez, V.; Sherban, M.; Charkoudian, J. *J. Am. Chem. Soc.* **1988**, *110*, 1498–1506.
(56) Warren, J. J.; Mayer, J. M. *J. Am. Chem. Soc.* **2010**, *132*, 7784–7793.
(57) Creutz, C. *Inorg. Chem.* **1981**, *20*, 4452–4453.